3-2023

Critical Infrastructure System Resiliency Modeling Using Multi-Layer Network Optimization

Spencer R. Figge

CRITICAL INFRASTRUCTURE SYSTEM RESILIENCY MODELING USING MULTI-LAYER NETWORK OPTIMIZATION

THESIS

Spencer R. Figge, Capt, USAF

AFIT-ENV-MS-23-M-191

DEPARTMENT OF THE AIR FORCE
AIR UNIVERSITY

AIR FORCE INSTITUTE OF TECHNOLOGY

Wright-Patterson Air Force Base, Ohio

AFIT-ENV-MS-23-M-191

CRITICAL INFRASTRUCTURE SYSTEM RESILIENCY MODELING USING MULTI-LAYER NETWORK OPTIMIZATION

THESIS

Presented to the Faculty

Department of Engineering Management

Graduate School of Engineering and Management

Air Force Institute of Technology

Air University

Air Education and Training Command

In Partial Fulfillment of the Requirements for the

Degree of Master of Science in Engineering Management

Spencer R. Figge, MBA

Capt, USAF

March 2023

AFIT-ENV-MS-23-M-191

CRITICAL INFRASTRUCTURE SYSTEM RESILIENCY MODELING USING MULTI-LAYER NETWORK OPTIMIZATION

Spencer R. Figge, MBA

Captain, USAF

Committee Membership:

Maj Brigham A. Moore, PhD, P.E., P.M.P.
Chair

Lt Col Benjamin R. Knost, PhD
Member

Lt Col Craig R. Poulin, PhD, P.E.
Member

AFIT-ENV-MS-23-M-191

Abstract

Accurately modeling the interdependent operation of critical infrastructure systems is an effective and efficient way of proactively evaluating system vulnerabilities and resiliency. Infrastructure systems are designed to transport essential commodities from where they are produced to where they are consumed and network flow-based models are one of the most effective ways to simulate and quantify infrastructure performance. The literature is populated with proposed models that must balance accuracy of interdependent operations, capability to include real-world considerations, and computational cost. This research proposes an alternative network-flow based model called the Critical Infrastructure System Resiliency Model (CISRM) that focuses on modeling a subset of operational interdependencies and allows user-input damage scenarios to include partial functionality of components, restrict the available repair resources, and limit the number of work crews available to make repairs. Due to the difficulties associated with obtaining real-world infrastructure data, this research demonstrated CISRM capabilities on a notional test network. The damage scenario simulations demonstrated the superiority of CISRM in quickly restoring infrastructure services when compared to alternative restoration prioritization heuristics. The simulations also show CISRM could be a powerful decision-making tool for weighing the costs and benefits of different levels of recovery investment and the potential impact on overall system resiliency.

Family, God, and Country

Acknowledgments

First, I would like to express my gratitude and appreciation to my wife and kids for their encouragement and tolerance through the early mornings, late nights, and long work hours put into classes and research over the last 18 months – they are the reason I was able to successfully complete this work. A special thanks to my wife in particular for her selfless dedication and unwavering support holding down the fort, not just at this assignment but through my previous and future assignments. I am incredibly grateful to have such a committed partner and have had the opportunity to share such a challenging and rewarding experience together. Second, I would like to thank Major Moore. The passion and energy you brought to the classes you taught and the research meetings we had were a tremendous source of motivation and encouragement throughout this challenging process. Next, I would like to thank my committee members, Dr. Chini and Lt Col Poulin. Dr. Chini, your classes, knowledge, and guidance were essential foundations upon which I was able to build a thorough understanding of my research area. Lt Col Poulin, your insights and research helped broaden the scope of my thinking and research from the theoretical realm to the real world and were much appreciated. Finally, I would like to thank my fellow classmates, the GEM class of 23M. I am incredibly thankful our paths crossed and we were able to form such tight bonds throughout this unique and challenging experience. I look forward to seeing you all again in the future.

Spencer R. Figge

Table of Contents

Page

List of Figures

List of Tables

CRITICAL INFRASTRUCTURE SYSTEM RESILIENCY MODELING USING MULTI-LAYER NETWORK OPTIMIZATION

I. Introduction

Improving the resilience of critical infrastructure systems (CISs) is essential due to the outsized societal, economic, and security impacts associated with infrastructure disruptions. CISs form the backbone of modern societies, providing a continuous flow of goods and services necessary for our common defense, economic security, and public health and safety (Department of Homeland Security, 2013). Society is becoming increasingly dependent on CISs, and CISs are functioning in an increasingly interconnected way such that any disruption in these services has the potential to cascade into a catastrophic disruption (Sharkey et al., 2015, 2016). Additionally, the frequency of CIS disruptions by natural and manmade disasters is increasing (Garay-Sianca & Nurre Pinkley, 2021a), and worldwide in 2020, natural hazards alone are estimated to have cause about $200 billion in economic losses (Jones et al., 2022). As such, there has been an increasing amount of research into mitigating vulnerabilities to and speeding up the recovery of CISs.

Much of the previous research involved creating mathematical models to simulate CIS operation to help identify critical components to protect, or provide an optimized prioritization of components to repair (Almoghathawi et al., 2019; González et al., 2016; Sharkey et al., 2015). Despite the numerous models that have been proposed, the nature of CISs, with their varying degrees of interdependency and multitude of ways to quantify resilience or performance, means that no single model will accurately depict all aspects or impacts from a disruption (Enayaty Ahangar et al., 2020). Additionally, mathematical modeling itself requires an inherent trade-off between comprehensiveness (i.e., the level of detail and factors included in the model), and the time, effort, and computational power required to run an analysis (Filippini & Silva, 2015; Ouyang, 2014).

One modeling approach that has been used is an economic-theory based approach in which infrastructures and their interdependencies are formulated as sectors in a Leontief input-output framework (Enayaty Ahangar et al., 2020; Haimes, Asce, Barry, Horowitz, Lambert, Asce, Santos, Crowther, et al., 2005; Ouyang, 2014). Haimes and Jiang (2001) proposed a physical-based inoperability input-output model in which the physical interconnections between infrastructure systems were modeled as production and consumption quantities of specific commodities (Haimes, Asce, Barry, Horowitz, Lambert, Asce, Santos, Lian, et al., 2005). By inputting a damage scenario as a degraded level of system performance, Haimes and Jiang were able to show the propagation of that disruption through the interdependent set of systems as an overall percent decrease in output (Haimes, Asce, Barry, Horowitz, Lambert, Asce, Santos, Crowther, et al., 2005). While this approach is effective at showing the risk to one system caused by a potential degradation in another on the macro-scale (Haimes, Asce, Barry, Horowitz, Lambert, Asce, Santos, Lian, et al., 2005), there is insufficient granularity in this approach to evaluate systems at the individual component level (Enayaty Ahangar et al., 2020; Ouyang, 2014) which is critical to informing resiliency investments and repair activities.

A second approach, which ultimately suffers from the same lack of granularity as the above-mentioned Leontief-based approach, is using a system engineering or system dynamics-based approach (Ouyang, 2014). This approach relies on input from subject matter experts to create a causal-loop diagram detailing the effects on one system based on a change or disruption in another (Ouyang, 2014). The Critical Infrastructure Protection/Decision Support Tool (CIP/DSS) is one example of a system dynamics-based tool created by the joint effort of several U.S.-based national laboratories to show the macro-scale consequences of CIS disruptions (Ouyang, 2014). While this may be useful for some purposes, determining actionable steps that can be taken to reduce specific system vulnerabilities or improve specific recovery procedures require component-level assessments, which this approach cannot provide (Ouyang, 2014).

The final methodology discussed here is using a network theory-based model. In network models, CISs are reduced to sets of nodes and arcs and can be assessed both topologically (i.e., based on the number and direction of connections between networked components) and functionally (i.e., by simulating whether or not a system is capable of supporting a sufficient flow of commodities) (Zarghami & Gunawan, 2021). For example, Lee et al. (2007) proposed the Interdependent Layer Network (ILN) model which uses a mixed-integer, flow-based model to generate a set of components to repair while seeking to minimize the cost of commodity flow and minimize unmet commodity demand. Cavdaroglu et al. (2013) expanded this work and proposed a alternative model that generates a list of components to repair, as well as provides an optimized repair schedule for the available repair crews, while minimizing the sum of flow costs, unmet demand costs, and the costs of restoration. Almoghathawi et al. (2019) constructed a multi-objective optimization problem that sought to identify and schedule restoration of damaged components while both maximizing the overall system resilience and minimizing the total system operating and repair costs. The increased functional details provided by these types of models allow them to identify critical components and optimize recovery prioritization (Ouyang, 2014). However, these increased capabilities come at the cost of increased complexity and are computationally expensive (Ouyang, 2014).

This research seeks to add to this body of knowledge by proposing a novel combination of network theory-based model capabilities that can provide CIS owners or emergency managers an alternative assessment of their system's vulnerabilities and resilience. The novel model proposed in this research is structured as a multi-objective optimization model which seeks to 1) maximize the overall resilience of an interdependent infrastructure system and 2) minimize the operating and restoration costs over a given time horizon. This model is unique in that it expands on a consolidated interdependency formulation proposed by Enayaty Ahangar et al. (2020), simplifying the model constraint equations, while also incorporating a resource-constrained restoration environment, and multiple component condition states allowing for different levels of component performance. When applied to a damaged network, the model generates an optimized repair prioritization of damaged components based on resource and work crew availability, that balances overall system resilience and total system costs.

The remainder of this article is structured as follows: Section 2 provides a more comprehensive analysis of previously proposed network models, specifically how CIS interdependencies are identified and modeled, and how infrastructure resilience has been defined and quantified. Section 3 describes the novel infrastructure model developed as part of this research including a detailed description of the notation used, the mathematical formulation, and the underlying assumptions. Section 4 provides an illustrative application of the proposed model by using it to evaluate the recovery of a simulated, multi-layer infrastructure network, in response to several damage scenarios. Finally, Sections 5 and 6 provide a discussion of the insights gained by the use of this new model, and a discussion of the limitations and potential areas of future research.

II. Literature Review

The previous section provided a high-level overview of some of the types of modeling approaches that have been used in evaluating infrastructure interdependencies and resilience. This section provides a more thorough discussion of previously developed network theory-based infrastructure models beginning with a discussion of the different types of CISs and which were of interest in this research. Following that is a discussion of different approaches to the classification and impact that interdependencies have on the functioning and recovery of CISs, and how previous models attempted to capture the influences of these interdependencies. This section concludes with a discussion of how previous models have attempted to measure cumulative infrastructure resiliency through the use of different performance metrics and resiliency curves.

Infrastructure Interdependencies

In 1997, the United States (U.S.) President's Commission on Critical Infrastructure Protection (PCCIP) identified eight CISs (i.e., telecommunications, power distribution, natural gas and oil distribution, banking and finance, transportation, potable water distribution, government services, and emergency services) of which the security, continuity, and availability were deemed an urgent priority (President's Commission on Critical Infrastructure Protection, 1997; Rinaldi et al., 2001). This Commission defined infrastructure as, "a network of independent, mostly privately-owned, man-made systems and processes that function collaboratively and synergistically to produce and distribute a continuous flow of essential goods and services," (President's Commission on Critical

Infrastructure Protection, 1997; Rinaldi et al., 2001). Since this first classification, understanding of what constitutes a CIS has evolved such that the U.S. Department of Homeland Security, in their latest National Infrastructure Protection Plan (NIPP) now lists 16 critical infrastructure sectors that should be safeguarded against disruption (Department of Homeland Security, 2013). The newest classification of CISs includes additions such as healthcare facilities, manufacturing facilities, food and agriculture sectors, and the defense industrial base (Department of Homeland Security, 2013). This expansion has led some in the field such as Sharkey et al. (2016) to draw the distinction between traditional civil infrastructure systems (i.e., power distribution, water distribution, transportation system, etc.) and social infrastructure (i.e., healthcare, food and agriculture, banking, etc.). This distinction has implications for the types of interdependencies that can exist between CISs and how they can be modeled. This research is primarily concerned with the traditional civil infrastructure systems most aligned with the PCCIP above (i.e., "a network of…man-made systems that function collaboratively…to produce a continuous flow of goods…" (President's Commission on Critical Infrastructure Protection, 1997)).

An important concept mentioned earlier and highlighted in the PCCIP definition above is the interdependent or collaborative nature of CISs. Interdependencies address the obvious reality that CISs do not exist and operate in a vacuum or an isolated manner, and what occurs in one infrastructure can directly or indirectly affect operations in another infrastructure system (Ouyang, 2014; Rinaldi et al., 2001). Additionally, when seeking to generate a model to evaluate and improve the resilience of a network of CISs to large-scale disruptions, the literature shows that modeling a single infrastructure system in isolation is often insufficient for formulating effective restoration plans (González et al., 2016; Sharkey et al., 2015). In order to obtain any realistic performance response and identify vulnerabilities and the recoverability of CISs, it is essential to include the impacts of interdependencies (Almoghathawi & Barker, 2019; González et al., 2016). As technology has advanced, the quantity and complexity of interdependencies between CISs has increased and is credited with improvements in CIS control and operational efficiency (Almoghathawi et al., 2019; Enayaty Ahangar et al., 2020; Ouyang, 2014). However, with these operational improvements come increased vulnerabilities as interdependencies increase the potential for cascading failures, or the ability of disruptions to propagate from one infrastructure system to another (Almoghathawi et al., 2019; Enayaty Ahangar et al., 2020; Ouyang, 2014).

Rinaldi et al. (2001) is often cited as the first work that provided a framework for categorizing different types of interdependencies between CISs. Rinaldi et al. (2001) posited four categories of interdependencies: physical, cyber, geographic, and logical. Physical and cyber interdependencies involve a physical or cyber linkage between infrastructure systems in which a commodity or information from one system is required as an input in another system. A geographic interdependency involves a simple colocation of components from two or more systems as in a utility corridor or communication and power cables being located on the same utility poles. Finally, the logical interdependency category acts as a catch-all and is defined as any link without direct physical, cyber, or geographic connections (Ouyang, 2014; Rinaldi et al., 2001).

As an alternative, Lee et al. (2007) utilized a five-category classification scheme of interdependencies: input dependence, mutual dependence, shared dependence, exclusive-or dependence, and colocation dependence. The input and mutual interdependencies utilized by Lee et al. (2007) are analogous to a one-way and two-way physical or cyber interdependency where one system relies on an input from another, or both systems rely on inputs from the other. The shared dependence category addresses the potential sharing of physical components between systems. The exclusive-or dependence addresses the potential sharing of an infrastructure system to provide multiple services where only one service can be provided at a time (i.e., a transportation network that cannot provide access for emergency services and access for the shipment of goods at the same time and location). Finally, the collocated dependence is simply a geographic colocation of multiple systems.

Taking the classification of interdependencies one step further, the classification schemes proposed in Rinaldi et al. (2001) and Lee et al. (2007) above, could themselves be considered a subset as operational interdependencies, meaning they can impact the daily operations of CISs (Garay-Sianca & Nurre Pinkley, 2021b; Sharkey et al., 2016). These operational interdependencies are responsible for cascading failures (Lee et al., 2007; Sharkey et al., 2016). Sharkey et al. (2016) proposed an entirely new category of interdependencies called restoration interdependencies, which they define as those that, “occur whenever a restoration task, process, or activity in one infrastructure is impacted by the restoration (or lack thereof) of another infrastructure,” (Sharkey et al., 2016). Restoration interdependencies will only exist when a large-scale disaster causes damage to multiple CISs and the timing of restoration tasks has the ability to impact restoration tasks in other systems (Sharkey et al., 2016).

The work by Sharkey et al. (2016) mentioned earlier brings up an important concept, that the list of applicable interdependencies will depend on the specific purpose of the model being created and the infrastructure systems being considered. In general, these CIS network models can be categorized by their intended use as either performance evaluation models, design models, mitigation models, or recovery models (González et al., 2016). Given the objective of enhancing overall CIS resiliency, this research focused on mitigation models, which centered around preparing or modifying systems to absorb disruptions, and recovery models, which focused on prioritizing the repair of failed components to restore system service (González et al., 2016). Additionally, this research focused on a subset of operational interdependencies and their potential to cause cascading failures across multiple CISs. Ouyang (2014) provides a review of several additional classification schemes of operational interdependencies and evaluates their ability to adequately classify a series of example interdependency scenarios. The results suggest that only the classification scheme from Rinaldi et al. (2001) was able to adequately sort all the potential examples, but this was likely due to the logical interdependency category (i.e., the catch-all category) which was responsible for classifying 60% of the example scenarios (Ouyang, 2014). However, the examples proposed by Ouyang (2014) included potential impacts on CISs such as emergency services, food and agriculture, and public transportation. These are considered to be social infrastructure systems, and are distinct from the traditional civil infrastructure systems that form the foundation of this research (Sharkey et al., 2016). This research was primarily concerned with interdependencies that only affected traditional civil infrastructure systems, and that could be adequately represented as a flow between two systems (i.e., physical and cyber or input and mutual dependence).

Quantifying Infrastructure Performance and Resilience

Having narrowed down the topics of interest for this research to disruption mitigation and recovery optimization models that consider a subset of operational dependencies, this section will now address how infrastructure performance and resilience have been evaluated in previous research, and how it was evaluated in this research. Numerous approaches have been proposed to quantify CIS resilience. Some of the most common methods used for quantifying resilience in network modeling include: 1) resiliency curves, which display a system performance metric across time, 2) measuring topological metrics of a networked system (i.e., node degree, node or arc betweenness, etc.), or 3) by evaluating other system characteristics that act as indirect measures of resilience such as robustness, reliability, redundancy, or risk (Almoghathawi et al., 2019; Poulin & Kane, 2021; Zarghami & Gunawan, 2021). The definition of resilience used in this research refers to four different system abilities: 1) the ability to prepare and plan for, 2) absorb, 3) recover from, and 4) adapt to future disruptions (National Research Council, 2012; Poulin & Kane, 2021). While network topological metrics, and measurements of redundancy, robustness, or risk can be helpful in evaluating a CIS's preparation for and absorption of a disruptive event, they are insufficient in evaluating an interdependent system's true vulnerabilities and operation (Alderson et al., 2015), something necessary to determine a system's ability to recover from a disruption. As such, resilience curves have emerged as one of the most effective methods to evaluate CIS resilience, and are the primary method utilized in this research. Almoghathawi et al. (2019) provide a visual representation of the different phases of system performance that should be considered when evaluating system resilience and generating a resiliency curve (Figure 1).

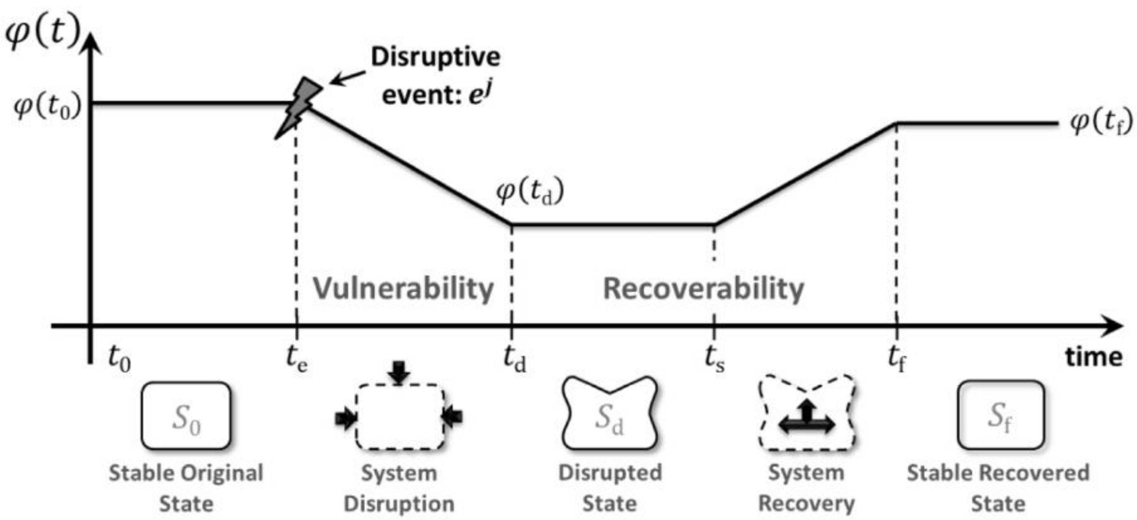

Figure 1: Example of resiliency curve showing system performance, $\varphi(t)$, through different phases of a disruptive event (Almoghathawi et al., 2019)

The fundamental purpose of CIS's, the provision of services or commodities for use by the general population or other infrastructure systems (Lee et al., 2007; Poulin & Kane, 2021). When there is a disruption, either physical or functional to a component of the system, it cannot provide its usual services at the required levels and there should be a measurable decrease in performance level (Lee et al., 2007). Poulin and Kane (2021) provide a discussion of several types of system performance metrics (i.e., $\varphi(t)$ in Figure 1) that can be utilized in resilience curves, as well as discussion of their strengths and weaknesses. Poulin and Kane (2021) identify three categories of infrastructure system performance metrics: 1) availability measures, 2) productivity measures, and 3) quality measures. Availability measures are the most commonly referenced metrics throughout the literature and describe the capacity or connectivity of an infrastructure system often via network topology metrics (Poulin & Kane, 2021). Productivity measures take into consideration the actual quantity of commodities or services provided by the system in terms of rate of flow or consumer demand met (Poulin & Kane, 2021). Finally, quality measures take more specific contextual factors into consideration to evaluate how well the services provided are satisfying specific consumer needs (i.e., water quality, travel time, etc.) (Poulin & Kane, 2021). From an engineering and modeling perspective, availability and productivity measures are the most applicable in evaluating infrastructure system resilience and are the primary categories of performance metrics utilized in this research.

This section concludes with a discussion of several previously proposed CIS mitigation and restoration models that provided the foundation for the current research, and how these previous models quantified infrastructure performance and resilience. First, Lee et al. (2007) constructed a model that measured system performance as the quantity of slack, or unmet demand, in a system, and tried to minimize the total system cost which included a penalty cost associated with slack. Slack was determined as the difference between baseline demand from a node and the quantity a system is able to supply in a degraded state (Cavdaroglu et al., 2013; González et al., 2016; Lee et al., 2007). While the work of Lee et al. (2007) successfully determines a set of components to repair while incorporating their five types of interdependencies, one critique is that their model, in that iteration, does not sequence the repairs or consider the assignment and scheduling of work crews (Almoghathawi et al., 2019). Cavdaroglu et al. (2013) expand on the work by Lee et al. (2007) while maintaining a similar measure of system performance, minimizing unmet demand. However, Cavdaroglu et al. (2013) produced a model that considers both the sequencing and scheduling of the restoration tasks not found in the Lee et al. (2007) work, and also incorporates restoration costs into the overall cost minimization objective function. González et al. (2016) constructed a similar model formulation relying on a penalty cost associated with unmet demand, but also included additional repair cost considerations associated with collocated components and site preparation (Almoghathawi et al., 2019). Enayaty Ahangar et al. (2020) proposed a slightly different measure of system performance, node functionality, as determined by the system's ability to deliver a sufficient quantity of commodities to meet the nodes demand, and awarded a bonus sum for each functional node.

Almoghathawi et al., (2019) adopted an alternative measure of resilience than the models discussed earlier, one proposed by Henry and Emmanuel Ramirez-Marquez (2012) who state that resilience is the ratio of recovered performance to total lost performance. In their formulation, system performance in their resilience equation is still quantified as a measure of slack (Almoghathawi et al., 2019). Additionally, Almoghathawi et al. (2019) add another component to their objective function, a cost minimization function, which includes a penalty cost associated with slack, creating a multi-objective optimization model that seeks to minimize cost and maximize resilience (i.e., minimize penalty costs associated with slack and maximize system performance recovered). On common factor in the models discussed in this section has been their reliance on a penalty cost for slack or bonus cost for node functionality, which is a common methodology for motivating mathematical models to repair components, for without an associated penalty, the cheapest solution for a cost minimization model is to not execute any repair functions (Almoghathawi et al., 2019; González et al., 2016; Moore, 2021). A critique of this penalty cost or bonus sum approach is that the they require appropriate scaling so as to not dominate the restoration optimization solution (Moore, 2021). To avoid the need for penalty or bonus costs, while still producing a model that tends towards repairing a damaged system, researchers could use competing objectives as Almoghathawi et al. (2019) did (Moore, 2021). However, the method for solving the multi-objective optimization problem selected by Almoghathawi et al. (2019) did not allow them to remove the penalty costs because their model ended up being totally motivated by the cost portion of their objective function, which alone, cannot tend towards repairing a system without the penalty motivator.

III. Methodology

This research proposes a novel, mixed-integer programming (MIP), multi-objective network optimization model, solved using a weighted sum approach that seeks to maximize overall system resilience while minimizing the costs to operate and repair the system. This novel model incorporates partial component (node or arc) functionality, proportional repair cost and resource consumption, infrastructure layer-specific work crews, and a consolidated commodity supply and demand formulation based on Enayaty Ahangar et al. (2020). This section details the underlying model assumptions, the notation utilized in this research, and the mathematical formulation of the Critical Infrastructure System Resiliency Model (CISRM) proposed in this research.

Assumptions

As with any optimization model, there are several underlying assumptions that must be considered when utilizing it. CISRM is no different. In this research, the underlying assumptions are:

- A critical infrastructure system can be reduced to a network of nodes and arcs that can be damaged or disrupted by various events (i.e., random failures, targeted attacks, natural disasters)
- Individual infrastructure layers can flow one or more services or commodities from supply nodes to demand nodes across a series of connected arcs
- In this formulation, each arc is only capable of flowing a single commodity at a time (i.e., no multicommodity flow)

- All nodes have a known supply or demand for each commodity considered in the simulation and all arcs have a known capacity for each commodity they transport
- The flow cost of a commodity across an arc is a known and fixed quantity
- Nodes that supply commodities can become disabled either by being physically damaged or by a failure of the system to provide sufficient commodities to meet the demand at that node
- Nodes and arcs can have partial functionality if damaged calculated as a proportion of baseline capacity as input by the user's damage simulation
- Partial damage to nodes does not affect the available supply or required demand of those nodes
- If a damaged component is restored, it is completely restored, there are no partial repair or recovery of function to anything less than the baseline level of performance
- No new arcs or connections can be constructed during the restoration process
- The quantities of critical resources necessary to fully repair each component are known and fixed quantities
- A work crew can only repair one component per time step
- Actual recovery durations are not considered, if a component is selected for repair in a given time step, it is assumed the component will be completely restored by the end of that time step

Notation

Table 1: Summary of CISRM notation

Notation	Description
$\mathcal{N}$	Set of all nodes
$\mathcal{A}$	Set of all arcs
$\mathcal{K}$	Set of all infrastructure layers
$\mathcal{L}$	Set of all commodities
$\mathcal{R}$	Set of all repair resources
$\mathcal{T}$	Set of all time steps
$\mathcal{N}'$	Set of all damaged nodes
$\mathcal{A}'$	Set of all damaged arcs
$d_{ik\ell}$	Demand (+) / Supply (-) parameter of commodity ℓ, by node i, in layer k
$u_{ij\ell}$	Capacity parameter of arc (i,j) for commodity ℓ
$c_{ij\ell}$	Cost parameter per unit flow of commodity ℓ across arc (i,j)
nf_{ir}	Quantity parameter of resource r required to repair (fix) node i
af_{ijr}	Quantity parameter of resource r required to repair (fix) arc (i,j)
$w_{k\ell}$	Work crews available to work on nodes in layer k or arcs for commodity ℓ
nv_i	Partial (percent) capacity parameter of node i after disruption
av_{ij}	Partial (percent) capacity parameter of arc (i,j) after disruption
q_r	Parameter for quantity available of resource r
μ_i	User-defined priority parameter of node i
$x_{ij\ell t}$	Variable quantity of commodity ℓ, flowing across arc (i,j), at time t
y_{ikt}	Variable flow state operability of node i, in layer k, at time t
nz_{it}	Variable damage state of node i and time t
az_{ijt}	Variable damage state of arc (i,j) at time t

This model notation begins with a network representation of an interdependent set of CISs, consisting of a set of nodes, $\mathcal{N}$, a set of arcs, $\mathcal{A}$, and a set of infrastructure layers $\mathcal{K}$, which are indexed as $i \in \mathcal{N}$, $(i,j) \in \mathcal{A}$, and $k \in \mathcal{K}$, respectively. To accurately depict multilayer set of infrastructure systems, this research utilizes a network-of-networks approach as the foundation of the proposed model instead of the alternative of using a multiplex structure. A multiplex structure is one in which each layer describes a single type of interaction or commodity and a node is reflected in each layer in which that node has a demand, supply, or transshipment function (Kivelä et al., 2013; Moore, 2021). Conversely, in a network-of-networks approach, each node is assigned to only one layer resulting in fewer nodes and arcs required to accurately depict system operation. For example, Figure 2 shows a model representation of a two-node, mutually dependent, two-layer system using both the multiplex approach (see panel a.), and the network-of-networks approach (see panel b.). In Figure 2, if node 1 is a water supply node that demands power, and node 2 is a power supply node that demands water, using the multiplex configuration would require four total nodes and four total arcs to represent this relationship. In contrast, the network-of-networks approach requires only one instance of each node, and one arc flowing in each direction.

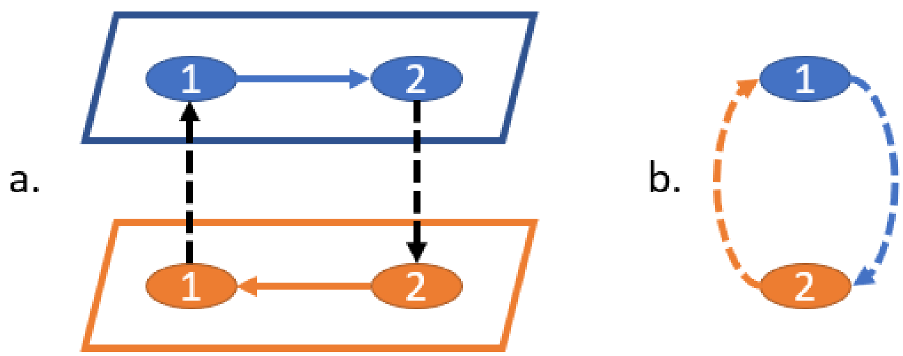

Figure 2: Example multiplex (a.) vs. network-of-network (b.) representation of a simple power and water supply interdependency

Utilizing the network-of-networks approach, each node belongs to a specific infrastructure layer (e.g., power distribution, water distribution, transportation, etc.), $\mathcal{K}$, and each arc transports a specific commodity (e.g., electricity, water, communication services, etc.), $\mathcal{L}$. The model also includes a set of resources, $\mathcal{R}$, that will be utilized in the repair of damaged network components (nodes or arcs), and a set of time steps, $\mathcal{T}$, over which a specific damage and recovery scenario can be analyzed.

Each node, representing a specific infrastructure layer component, can supply or demand a quantity of each commodity considered in the model. This parameter is denoted as $d_{ik\ell}$ in which a negative value signifies a supply of commodity $\ell \in \mathcal{L}$, at node $i \in \mathcal{N}$, in layer $k \in \mathcal{K}$, and a positive value signifies a demand of that commodity. In addition, each arc between nodes has a maximum capacity of a commodity that can transit across that arc at a given time. The maximum arc capacities across arc $(i,j) \in \mathcal{A}$ of commodity $\ell \in \mathcal{L}$ are denoted by $u_{ij\ell}$. Finally, to aid in estimating the operating expenses of each infrastructure layer, there is a unit flow cost associated with flowing any commodity throughout the network. This flow cost is denoted as $c_{ij\ell}$ and represents the cost to flow one unit of commodity $\ell \in \mathcal{L}$ across arc $(i,j) \in \mathcal{A}$.

When inputting a specific damage scenario into the model, there are a number of additional parameters or factors that can be included in the formulation. First, the sets of damaged nodes and damaged arc that will begin the simulation with some sort of diminished operating capacity are annotated as $\mathcal{N}' \subseteq \mathcal{N}$ and $\mathcal{A}' \subseteq \mathcal{A}$. When entering a component into the set of damaged nodes or arcs, the user has the option to assign a parameter to the node, nv_i, or arc, av_{ij}, which allow for partial functionality (on a scale of 0-1 or 0% to 100%) of the given components as detailed in the constraint equations below. The user can also input the available quantity or maximum resource limits of the critical resources, q_r, which can be utilized by work crews to repair damaged components. Users can also set an external prioritization value for each node, μ_i, such that the model will prioritize repair of and restoration of services to higher rated nodes first.

When considering the repair or restoration of network components, each node or arc requires a known quantity of key resources (contained in set $\mathcal{R}$) that it would take to restore the node or arc to full functionality. These quantities are denoted by the parameters nf_{ir} and af_{ijr} which are the resources required, $r \in \mathcal{R}$, for repair of node $i \in \mathcal{N}'$, and arc $(i,j) \in \mathcal{A}'$, respectively. Additionally, there are a limited number of work crews available for each infrastructure layer $k \in \mathcal{K}$ or commodity $\ell \in \mathcal{L}$, denoted by the parameter $w_{k\ell}$.

Finally, there are several variables present in the model that allowing for a number of different solutions to exist for a given scenario. First, $x_{ij\ell t}$ represents the quantity of flow of commodity $\ell \in \mathcal{L}$, across arc $(i,j) \in \mathcal{A}$, at time $t \in \mathcal{T}$. Second, y_{ikt} is a binary flow-state operability variable that takes a value of 1 if node $i \in \mathcal{N}$ and layer $k \in \mathcal{K}$ has been supplied with enough commodities to satisfy all its demands, and 0 if at least one commodity has not been supplied in sufficient quantity. The last two variables are nz_{it} and az_{ijt} which are also binary and indicate whether a node or an arc were disrupted in the damage simulation (i.e., nz_{it} or $az_{ijt} = 0$) and available to be repaired by the work crews, or if they were not damaged (i.e., nz_{it} or $az_{ijt} = 1$).

Mathematical Model

The proposed model seeks to balance two conflicting objectives: system resilience and system cost. These objectives are competing because an increase in resilience (desired) corresponds with an increase in cost (not desired). In this research, system resilience, φ, was defined as the number of operable nodes (i.e., nodes with $y_{ikt} = 1$), multiplied by the criticality of those nodes, μ_i, summed across all infrastructure layers and across time, shown in Equation 1. This resilience metric takes into consideration both the damage state of given nodes and the meeting of commodity demands at those nodes (i.e., the node itself must be repaired and the overall system must be repaired to the extent required to be able to supply the required commodities to a node, in order for that node to be functional).

$$\varphi = \sum_{i \in \mathcal{N}} \sum_{t \in \mathcal{T}} \sum_{k \in \mathcal{K}} y_{ikt} * \mu_i \qquad (1)$$

There were three components that added to the total system cost considered in this research, commodity flow cost, node repair cost, and arc repair cost, with total cost being the summation of the three, across all layers, commodities, and time steps. In this formulation, cost was calculated as the sum of the money required to repair the damaged nodes and arcs, Equation 2, with "money" being considered as one of the critical resources listed in the set, $\mathcal{R}$.

$$\mathcal{C} = \sum_{t \in \mathcal{T}} \left(\sum_{\ell \in \mathcal{L}} \sum_{(i,j) \in \mathcal{A}} x_{ij\ell t} * c_{ij\ell} + \sum_{i \in \mathcal{N}'} nz_{it} * nf_{i'money'} + \sum_{(i,j) \in \mathcal{A}'} az_{ijt} * af_{ij'money'} \right) \tag{2}$$

The objective function was solved using a weighted-sum method to balance the competing objectives of maximizing system resilience, φ, while minimizing total cost, $\mathcal{C}$. Since resilience is to be maximized and cost is to be minimized, $\mathcal{C}$ is subtracted from φ to motivate the model to increase φ and decrease $\mathcal{C}$. To do this, a weight, ω, is set by the user which allows for evaluating numerous solutions based on varying degrees of prioritization between the objectives (e.g., if maximum resilience is desired, ω is set to 1 or if a maximum resilience and minimum cost are valued equally, ω would be set to 0.5). The user may also input a scaling factor, λ, to compensate for the potential differences in order of magnitude between φ and $\mathcal{C}$. This yields an overall objective function given in Equation 3.

$$MAX \left(\omega * \varphi - \frac{1 - \omega}{\lambda} * \mathcal{C} \right) \tag{3}$$

As mentioned previously, the model is subject to a number of categories of constraints that limit the potential solutions and govern the functioning of the system. The first constraint listed below is the flow-balance constraint, Equation 4, adapted from Enayaty Ahangar et al. (2020) which allows for a more concise formulation while still maintaining the ability to simulate many interdependent relationships.

$$\sum_{(i,j)\in\mathcal{A}} x_{ij\ell t} - \sum_{(j,i)\in\mathcal{A}} x_{ij\ell t} \leq -d_{ik\ell} * y_{ikt}, \forall\, i \in \mathcal{N}, k \in \mathcal{K}, \ell \in \mathcal{L}, t \in \mathcal{T} \quad (4)$$

The following constraints govern the quantities of the commodities that can flow from one node to another based on the capacity and damage state of the arc itself (Equation 5), the damage state of the origin node (Equation 6), and the damage state of the destination node (Equation 7), respectively. The partial functionality capabilities of CISRM are based on the work of Almoghathawi and Barker (2019). The fundamental theory behind the constraints in Equations 5-7 is that if a component is going to have a partial functionality (i.e., nv_i or $av_{ij} < 1$), that component will be in the set of damaged components and have a damage state of 0 (i.e., nz_{it} or $az_{ijt} = 0$), indicating it can be repaired by the available work crews.

$$x_{ij\ell t} \leq u_{ij\ell} * \left(\left(1 - az_{ijt}\right) * av_{ij} + az_{ijt}\right), \forall\, (i,j) \in \mathcal{A}, \ell \in \mathcal{L}, t \in \mathcal{T} \quad (5)$$

$$x_{ij\ell t} \leq u_{ij\ell} * \left((1 - nz_{it}) * nv_i + nz_{it}\right), \forall\, i \in \mathcal{N}, (i,j) \in \mathcal{A}, \ell \in \mathcal{L}, t \in \mathcal{T} \quad (6)$$

$$x_{ij\ell t} \leq u_{ij\ell} * \left(\left(1 - nz_{jt}\right) * nv_j + nz_{jt}\right), \forall\, j \in \mathcal{N}, (i,j) \in \mathcal{A}, \ell \in \mathcal{L}, t \in \mathcal{T} \quad (7)$$

The next set of constraints govern the repair and restoration of damaged components. The first constraint in this subset restricts the number of components that can be repaired per time step to the number of work crews assigned to that layer, Equation 8. As mentioned earlier, work crews can be assigned to both an infrastructure layer, $k \in \mathcal{K}$, and a commodity layer, $\ell \in \mathcal{L}$. This is because in this formulation, nodes are associated with a specific infrastructure layer while arcs are associated with the commodity or commodities that flow across them, and work crews should be able to repair either nodes or arcs within a given system (i.e., if $w_{k\ell} = w_{(power)(electricity)} = 2$, each of the two work crews could repair a node associated with the power distribution layer or an arc associated with the flow of electricity).

$$\sum_{i \in \mathcal{N}'} nz_{it} - nz_{i(t-1)} + \sum_{(i,j) \in \mathcal{A}'} az_{ijt} - az_{ij(t-1)} \leq w_{k\ell}, \forall\, k \in \mathcal{K}, \ell \in \mathcal{L}, t \in \mathcal{T} \tag{8}$$

The next constraint, Equation 9, restricts the number of components that can be repaired based on the number of available critical resources by summing the number of critical resources that would be consumed by repairing a given component. This constraint also allows for proportional resource consumption to be factored in based on the partial damage or capacity of components input by the user's damage scenario.

$$\sum_{t \in \mathcal{T}} \left(\sum_{i \in \mathcal{N}'} nf_{ir} * (1 - nv_i) * \left(nz_{it} - nz_{i(t-1)}\right) + \sum_{(i,j) \in \mathcal{A}'} af_{ijr} * \left(1 - av_{ij}\right) * \left(az_{ijt} - az_{ij(t-1)}\right) \right) \leq q_r, \forall\, r \in \mathcal{R} \tag{9}$$

The following two constraints simply maintain the restored status of damaged nodes, Equation 10, and arcs, Equation 11, over the duration of the damage scenario.

$$nz_{it} - nz_{i(t-1)} \geq 0, \forall\, i \in \mathcal{N}', t \in \mathcal{T} \tag{10}$$

$$az_{ijt} - az_{ij(t-1)} \geq 0, \forall\, (i,j) \in \mathcal{A}', t \in \mathcal{T} \tag{11}$$

The last constraints listed below are non-negativity constraints and binary constraints restricting the signs and values of their respective parameters or variables. Equation 12 sets the non-negativity of commodity flow, and Equations 13, 14, and 15 set the binary limitations for node flow state, node damage state, and arc damage state, respectively.

$$x_{ij\ell t} \geq 0, \forall\ (i,j) \in \mathcal{A}, \ell\ \in \mathcal{L}, t \in \mathcal{T} \tag{12}$$

$$y_{ikt} \in \{0,1\}, \forall\ i \in \mathcal{N}, k \in \mathcal{K}, t \in \mathcal{T} \tag{13}$$

$$nz_{it} \in \{0,1\}, \forall\ i \in \mathcal{N}, t \in \mathcal{T} \tag{14}$$

$$az_{ijt} \in \{0,1\}, \forall\ (i,j) \in \mathcal{A}, k \in \mathcal{K}, t \in \mathcal{T} \tag{15}$$

IV. Results

Illustrative Example

A test network was utilized to demonstrate the functionality of CISRM and its ability to evaluate the performance and optimal restoration of an interdependent infrastructure network. The test network is a two-layer, 18-node network, consisting of nine nodes in the power distribution layer, and nine nodes in the water distribution layer. The network itself was adapted from the work of Almoghathawi and Barker (2019) and expanded to include additional parameters such as flow cost, arc capacities, supply and demand quantities, and component repair resource requirements, which are detailed in Appendix 1. This section further describes the test network, the various damage simulations the network was subjected to and CISRM was used to evaluate, and displays the results.

Test Network

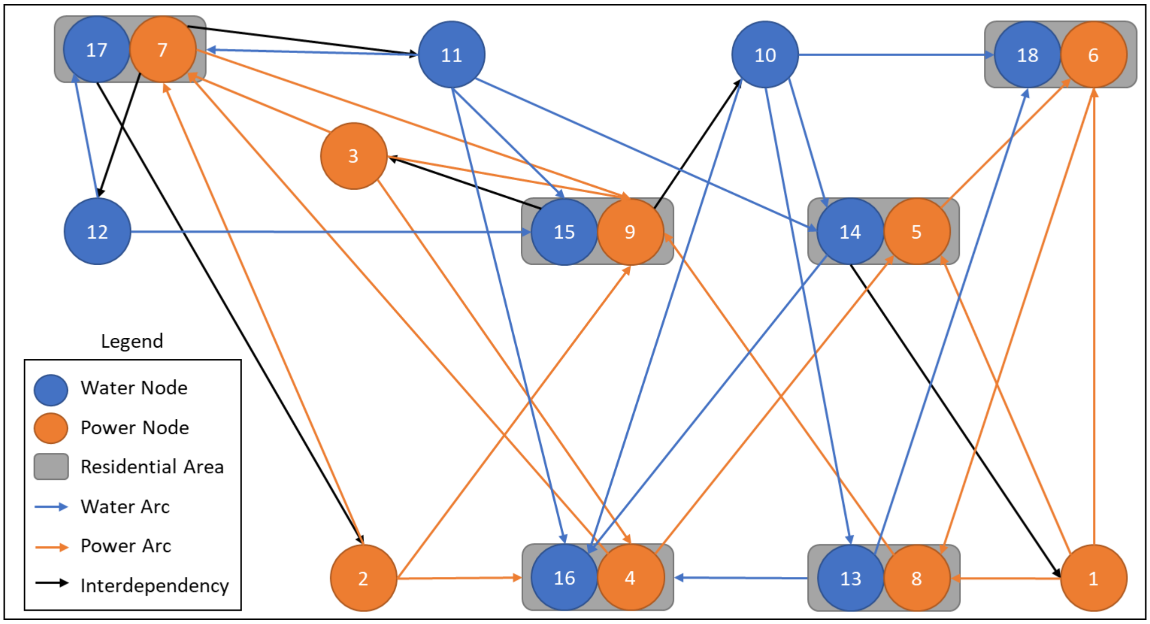

Figure 3: Test network used for evaluation of CISRM capabilities

The test network utilized in this research was a two-layer, interdependent infrastructure network, consisting of nine power distribution nodes, nine water distribution nodes, and various intra- and inter-layer arcs completing the network, shown in Figure 3. There were three power supply nodes (nodes 1, 2, and 3) and three water supply nodes (nodes 10, 11, and 12). The other six nodes from each layer were grouped together to simulate a residential area with both a power demand and a water demand. Additionally, interdependencies exist between the water distribution layer and the power supply nodes, which require water to generate and supply electricity, and the power distribution layer and the water supply nodes, which require electricity to supply water to the system.

Damage Scenarios

Previous research identifies three common sources of potential disruptions for CISs: random failures, malevolent attacks, and natural disasters (Alkhaleel et al., 2022; Almoghathawi et al., 2019; Ouyang, 2017). The damage scenarios selected for this research were modeled after these three potential sources and adapted to take into consideration the small size of the test network. The first damage scenario utilized in this illustrative example was a total failure scenario in which all components, nodes and arcs, were damaged and at 0% functionality. In this scenario, the weight, ω, was set at 1, to maximize system resilience in recovery. The second damage scenario began with a fully functional and fully connected network and looked at degradation in system performance as one component in each layer was damaged sequentially. This damage pattern mimics some behavior of malevolent attacks. The final damage scenario was a random failure scenario, similar to a natural disaster, in which a random number between zero and one was generated for each component, and if that number was less than 0.5, then that component was said to be damaged with a percent operability equal to that randomly generated number.

Simulation Results

All tests and simulations conducted as part of this research were executed on a laptop computer using an Intel i5-8250U CPU @ 1.60 GHz with 8.00 GB RAM. This research used GAMS Studio software, specifically GAMS Studio 1.8.2 64-bit, and relied on the IBM ILOG CPLEX 20.1 solver to execute the mixed-integer programming

CISRM model. The GAMS code generated as part of this research is included in its entirety in Appendix 2. Although computational efficiency was not the focus of this research, it should be noted that the longest computational time associated with solving any of the optimization problems discussed was 35 minutes.

Before CISRM could be applied to the desired damage scenarios, certain user-defined values needed to be determined, mainly the appropriate weighting factors (ω) and scaling factors (λ) necessary to generate the best set of feasible solutions. No external prioritizations, μ, were assigned to any of the nodes during any of these simulations (i.e., $\mu_i = 1, \forall\ i \in \mathcal{N}$). Both ω and λ can have a significant impact on the results of the model so a sensitivity analysis was done as part of this research to determine the values that worked best for the input test network data. Given its presence in the resilience-focused objective function, if μ values were assigned to components, they would also impact the analysis and should be included in any sensitivity analysis. If CISRM were applied to an alternate network, it is likely a similar analysis would have to be done until a range of acceptable input values could be determined for which precalculated values of ω and λ would be sufficient. For this analysis various combinations of ranges for ω and values of λ were input into the model and used to generate Pareto fronts, which are graphical representations of the optimal solutions to multi-objective optimization problems. The best combination of values for ω and λ would yield a diverse set of optimal solutions, indicated by the number and spacing of the solutions along the Pareto front. Appendix 3 contains the total set of results generated during the sensitivity analysis, but for this research, ω was constrained to the range of 0-1 while λ was set to 5000. The rest of this section describes the actual results generated from the damage scenarios.

Figure 4 shows the prioritization of the components to repair in both the power and water layer of the test network based on CISRM recommendations, columns 1 and 2, and a recommendation based on a network topological prioritization, columns 3 and 4. Figure 5 is a partial resilience curve showing the trajectory of system recovery with the x-axis being time steps in the model and the y-axis being system performance measured as a percentage of functional nodes compared to the baseline (i.e., nodes must be both physically repaired and be supplied with a sufficient quantity of commodities to meet their demands). System recovery in Figure 5 is shown with components being repaired per the recommendations of the CISRM (i.e., "CISRM" lines), and based on the topological recommendations (i.e., "topology" lines). In addition to the CISRM vs. topological comparison, Figure 5 also shows recovery trajectory when considering only one work crew per infrastructure layer (i.e., "1 WC" lines) and two work crews per infrastructure layer (i.e., "2 WC" lines). Figure 6 shows the total cost across the recovery horizon for each of the four scenarios stated earlier: 1 work crew – CISRM model prioritization, 2 work crew – CISRM model prioritization, 1 work crew – topological prioritization, and 2 work crew – topological prioritization.

#	Power (CISRM)	Water (CISRM)	Power (Topology)	Water (Topology)
1	Arc 3-7	Node 11	Arc 9-10	Node 10
2	Node 3	Arc 11-15	Node 9	Arc 14-1
3	Arc 7-11	Arc 15-3	Node 7	Arc 15-3
4	Node 7	Node 15	Arc 8-9	Arc 17-2
5	Arc 7-12	Node 12	Arc 7-11	Node 14
6	Node 4	Arc 12-15	Node 2	Arc 10-14
7	Arc 3-4	Arc 11-14	Node 3	Node 11
8	Arc 4-7	Node 14	Node 8	Arc 11-14
9	Node 5	Node 17	Arc 6-8	Node 15
10	Arc 2-4	Arc 11-17	Node 1	Node 17
11	Node 2	Arc 17-2	Arc 5-6	Arc 10-13
12	Arc 4-5	Arc 12-17	Arc 4-5	Arc 10-18
13	Node 9	Arc 10-13	Arc 1-8	Arc 12-15
14	Arc 3-9	Node 13	Arc 2-7	Arc 12-17
15	Arc 9-10	Node 10	Arc 3-7	Arc 11-15

Figure 4: Table showing the order of top 15 components to be repaired based on CISRM prioritization and topological-based recommendations for the total failure scenario

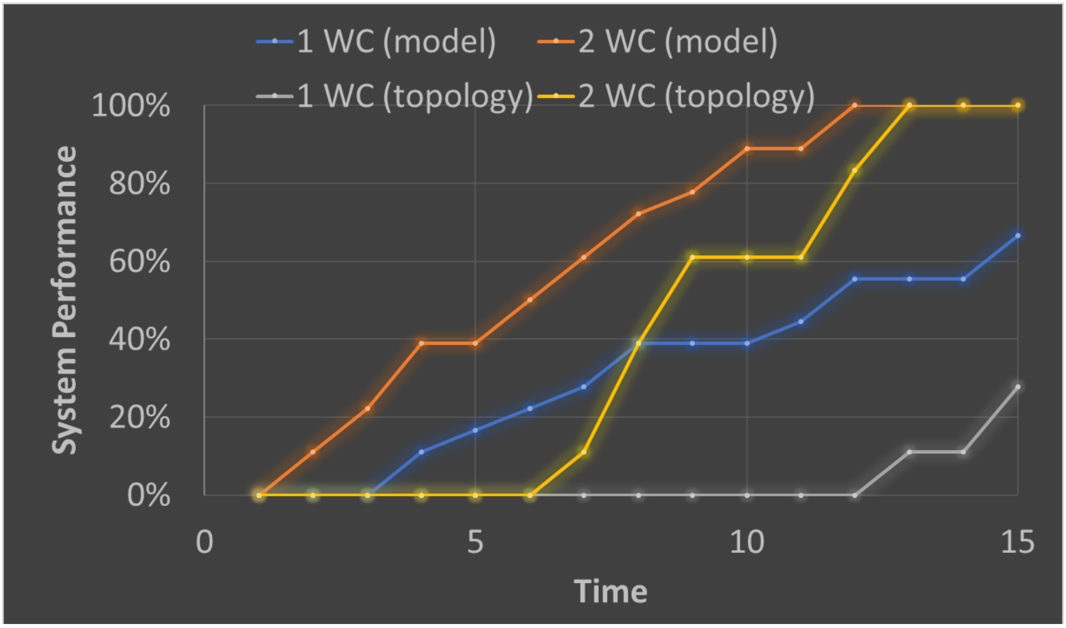

Figure 5: Partial resilience curve showing system recovery trajectory for the total failure scenario in response to four different repair prioritization scenarios

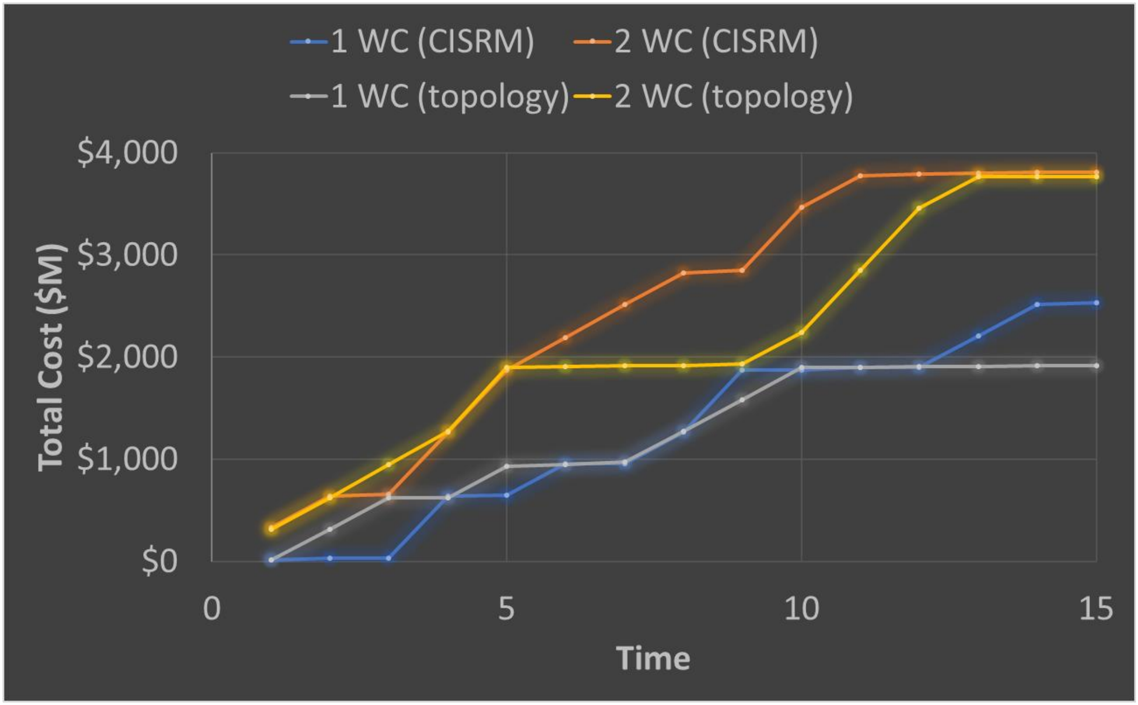

Figure 6: Repair costs for the total failure scenario across the time horizon based on four different repair prioritization scenarios

Figures 7-9 pertain to the second damage scenario, the targeted attack. As mentioned earlier, the network in this scenario began with all components connected as shown in Figure 3 and operating at 100% functionality. One component was removed from each network layer (i.e., one power arc or node and one water arc or node) in succession and the total number of components removed from each layer is shown on the horizontal axis of Figures 7-9. The components were removed in the same order or prioritization as shown in Figure 4 with the top component being removed first and then moving down the list. Figure 7 shows total system power flow as a percentage of the baseline level as components are successively removed from each infrastructure layer.

Figure 8 shows total system water flow as a percentage of baseline as system components are removed as described above. Finally, Figure 9 shows overall system performance as measured by the percentage of functional nodes compared to the baseline as components are targeted and removed from the system.

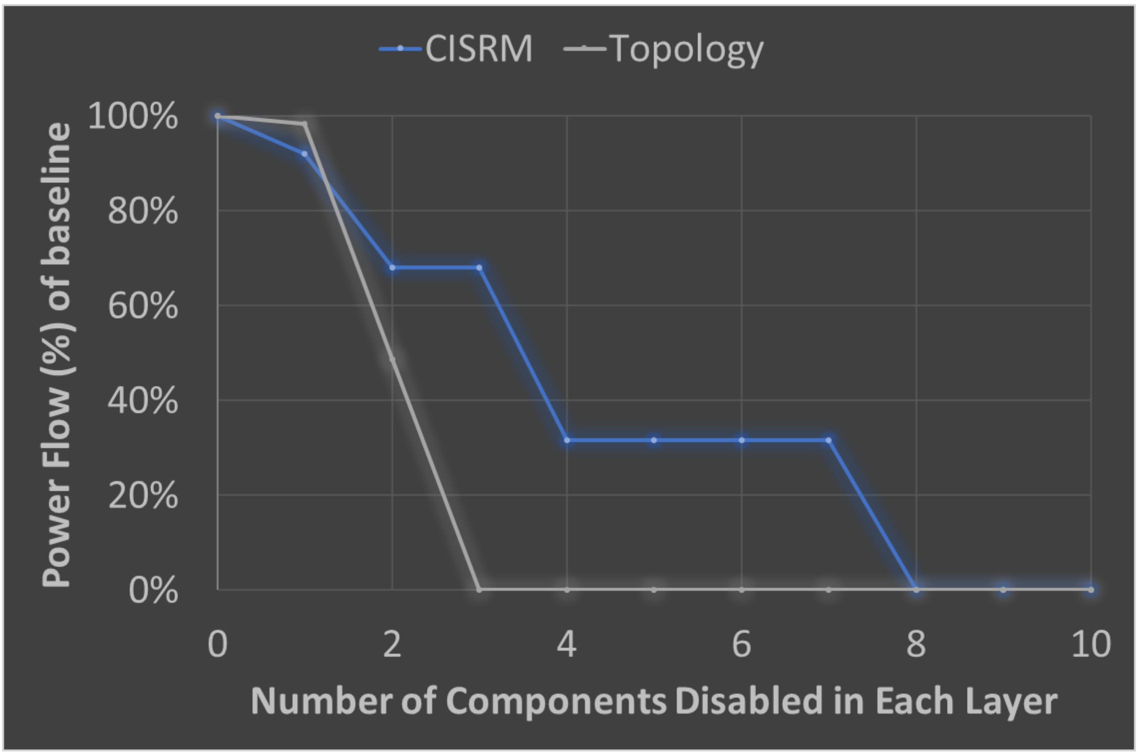

Figure 7: Total system power flow as a percentage of baseline (y-axis) as an increasing number of components are removed from both infrastructure layers (x-axis)

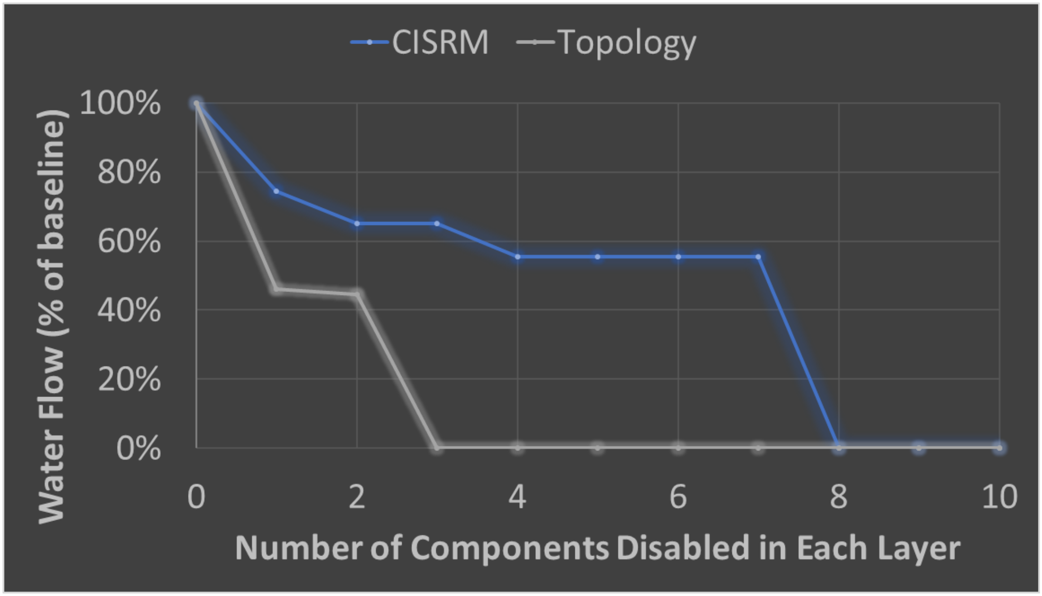

Figure 8: Total system water flow as a percentage of baseline (y-axis) as an increasing number of components are removed from both infrastructure layers (x-axis)

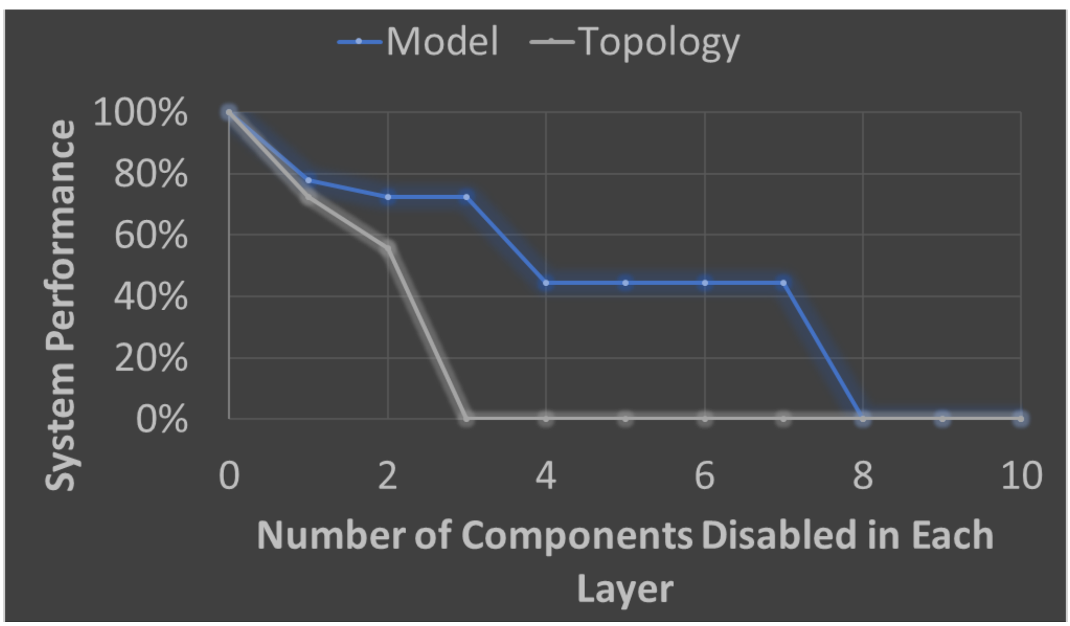

Figure 9: Overall system performance measured as a percentage of functional nodes (y-axis) as an increasing number of components are disabled in both of the interdependent infrastructure layers (x-axis)

Figure 10 shows a table of damaged components and their percent of baseline functionality as generated using the random failure scenario procedure noted above. For example, the random number generated for component "Node 1" was 0.3 which was under the 0.5 threshold used for determining whether or not a component was damaged. Therefore, "Node 1" was said to be operating at 30% of its baseline capacity. These damaged components were then input into the CISRM model which then prioritized component repair based on several weighting factors (i.e., values of ω in Equation 3). Figures 11 and 12 show system performance as a percentage of functional nodes and total costs, respectively, as the total system is repaired. This scenario only utilized one work crew for each infrastructure layer (i.e., a maximum of one component could be repaired from each layer at each time step). The three values of ω used in this scenario were 0.3, 0.45, and 0.9. As shown in Equation 3, as ω increases, so does the emphasis on system resilience as compared to total costs.

Damaged Component	Functional Capacity (%)	Damaged Component	Functional Capacity (%)
Node 1	30	Arc 7-11	10
Node 2	30	Arc 7-12	0
Node 4	20	Arc 9-10	10
Node 7	40	Arc 10-13	10
Node 10	40	Arc 10-14	40
Arc 1-6	10	Arc 10-16	0
Arc 2-4	20	Arc 11-14	0
Arc 4-7	0	Arc 11-16	30
Arc 5-6	40	Arc 12-15	10
Arc 6-8	10	Arc 12-17	0
Arc 7-9	40	Arc 14-16	20

Figure 10: Table showing damaged components and their percent of baseline functionality used in the random failure damage scenario

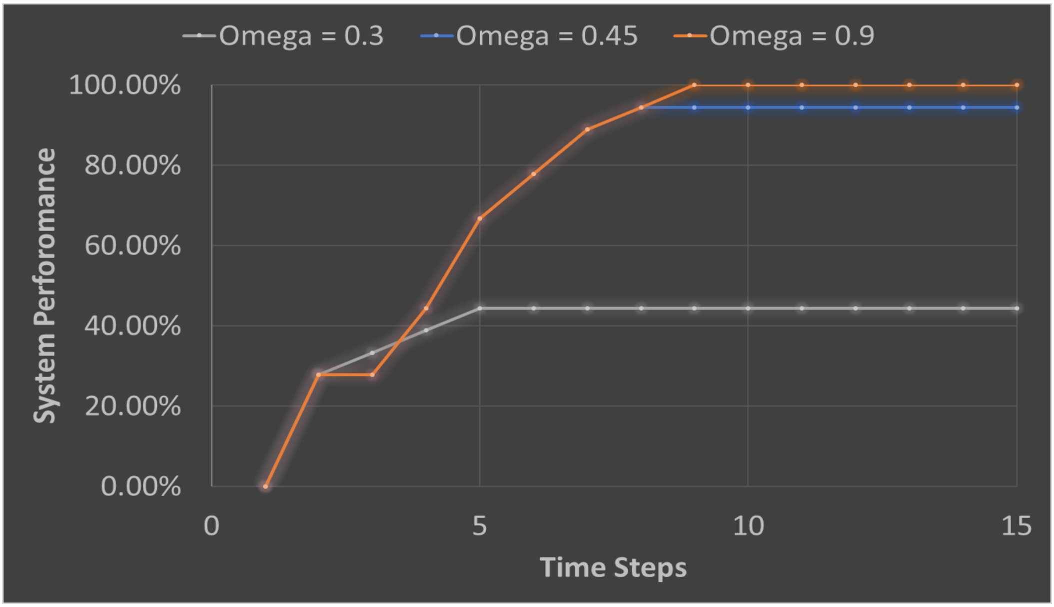

Figure 11: Partial resilience curve showing system recovery trajectory for the random failure scenario using three different ω values in the CISRM

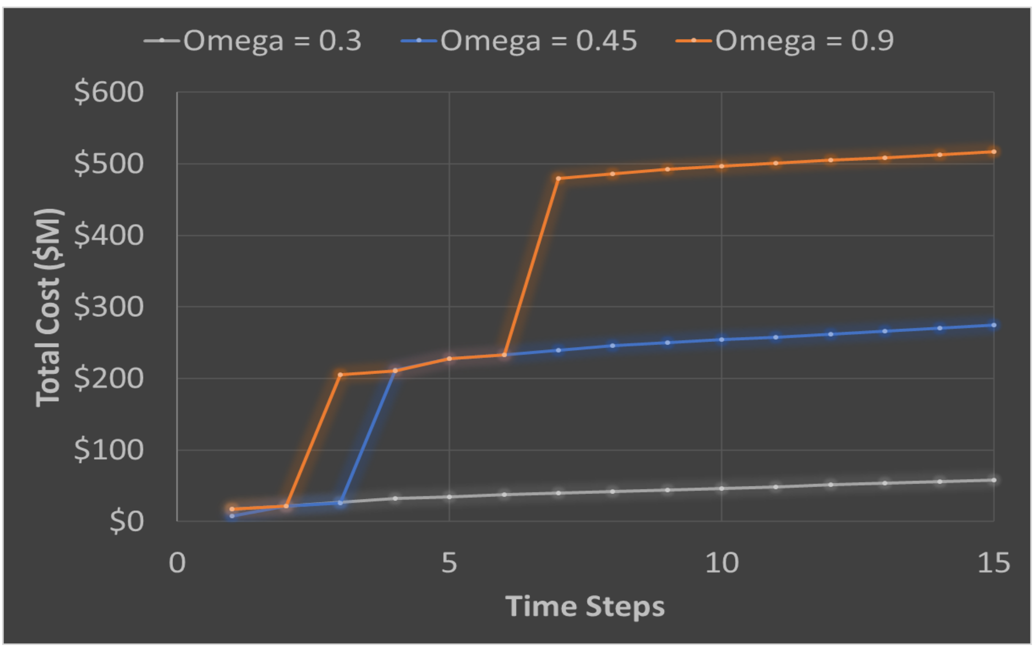

Figure 12: Total costs over time for the three random failure recovery scenarios described above and shown in Figure 10

V. Discussion

This section discusses the results of the illustrative example described earlier and how they demonstrate the functionality of CISRM. This section follows the layout of the previous section by first discussing the total failure scenario, followed by the targeted attack scenario, and finishes with a discussion of the random failure scenario.

Total Failure Scenario

From the total failure scenario evaluated in Figures 4-6, it can be seen that the CISRM proposed a more optimal recovery than the alternative based solely on betweenness centrality. Figure 4 shows the order in which the first 15 components in each layer were repaired based on the CISRM model and based on network topology. Due to the notional nature of the test network, all components (18 nodes and 34 arcs) were required to achieve 100% resiliency meaning that a one work crew per infrastructure layer scenario would require 27 time steps to complete total reconstruction of the network. Of note is the fact that CISRM, under both the one and two work crew scenarios repaired the same components early in the recovery. The repaired components at each time step were recorded after running CISRM and used to generate the prioritization shown in columns one and two of Figure 4. The topological metric used in this research was betweenness centrality, which is a measure of the number of shortest paths between all nodes that flow through a specific node or arc (Dunn et al., 2013). Betweenness centrality provided a consistent topological metric that could be applied to both nodes and arcs as opposed to other topological metrics such as degree which would just prioritize nodes. Betweenness centrality was calculated for the network as a whole, as shown in Figure 3, and the values were separated into their respective layers to generate the prioritizations shown in columns three and four of Figure 4. Complete betweenness centrality values are included in the test network data provided in Appendix 1. In both the one work crew and two work crew scenarios, CISRM achieved a higher level of resilience in fewer time steps than the topological prioritization. As shown in Figure 5, in the two-work crew scenario, both CISRM and the topological method achieved 100% system performance at 12 time steps and 13 time steps, respectively. However, the first fully functional node (i.e., repaired and receiving sufficient commodity supply) appears much sooner with CISRM than with the topological approach, the second time step as opposed to the seventh. Likewise, in the one work crew scenario, CISRM achieves its first functional node at the fourth time step whereas the topological approach does not achieve a functional node until time step 13. This shows that using CISRM to prioritize repairs leads to a more resilient system, measured as cumulative system performance over the time horizon.

Figure 6 shows the total costs incurred in each scenario from both system operation and recovery. This CISRM application had an ω value of 1 meaning it would simply try to optimize system resilience with no regard for minimizing total costs. Additionally, since both the two-work crew CISRM and topological approaches achieved 100% resilience, their total costs are similar because they eventually repaired all the same components and repair costs remained constant throughout. However, the two-work crew – CISRM approach has a slightly higher total cost than the two work crew – topological approach because of increased level of system functionality achieved early on and the associated increased flow costs. In general, flows cost in this particular example were drastically overshadowed by the repair costs and did not significantly influence these results.

From the total failure scenario, it can be seen that the CISRM is significantly more efficient at recovering a damaged interdependent infrastructure system than betweenness centrality. This is because of the interdependent nature of the system and the inability of the betweenness centrality metric to distinguish between water nodes and power nodes and water arcs and power arcs. This inability results in a failure to effectively capture system performance and functionality as measured by the delivery of specific commodities to their required destinations. On the other hand, CISRM provides the most efficient recovery prioritization based on system performance and functionality and lays out the bare minimum needed to have a fully connected and operational network. There were additional components that were not prioritized for repair by CISRM because they were redundant and did not offer additional performance enhancements. This scenario further demonstrates the capabilities of CISRM to project recovery trajectories using multiple work crew scenarios. However, as the model is currently configured, it does not capture important work crew considerations such as the cost to hire, train, and equip additional work crews which would need to be considered in a cost optimization scenario.

Targeted Attack Scenario

The total failure scenario discussed earlier sought to identify the critical components that needed to be repaired in order to reconstruct a fully disabled system. The targeted attack scenario sought to also identify critical components, but takes an alternative approach beginning with a fully connected and functional system, and removing individual components in succession and evaluating the degradation in service. The same prioritization schemes from Figure 4 were used in this scenario, but instead of being repaired, the components were removed from the system starting from the top and moving down. The idea being that, the components identified for repair first, by both CISRM and by topology, were the most critical for system operation, and disrupting those components first would have the greatest impact in overall system degradation.

Figure 7 shows how the power flow through the whole system drops as components are removed from each layer of the infrastructure. It shows that, by removing the components based on the topological prioritization, only three components need to be removed from each network to cause a total system failure resulting in 0% power flow. Conversely, when targeting components based on the CISRM prioritization, eight components needed to be removed from both layers to cause a total cessation of power flow. Likewise, Figure 8 shows the same results but from the perspective of total water flow through the network. Finally, Figure 9 shows total system performance measured as percentage of operational nodes as compared to the baseline. Figure 9 reveals that by removing three components in order of the topological prioritization, and eight components based on the CISRM prioritization, all the nodes in the network were rendered nonfunctional. By looking at the actual degradation curve in Figure 9, it can be seen that when only the top two components are removed, the system is still able to maintain 58% functionality when looking at the topological targeting, and 76% functionality when looking at the CISRM-based targeting.

Based on the results in Figure 7-9, targeted attacks on this network appear to be more effective when based on topological metrics than when based on the CISRM repair prioritization. This is likely a function of the small size of the test network and the outsized effect that removing a single node can have on overall connectivity. However, it can be useful in identifying potential candidates for hardening or redundancies in order to mitigate the potential impacts to the system from component failures. Conversely, these results could also inform adversaries that targeting interdependent infrastructure systems based on topological metrics yields a faster degradation in service than alternative targeting prioritizations.

Random Failure Scenario

The random failure scenario depicts a probabilistic disruption event such as a natural disaster. Figure 10 displays the results of the random number assignment process showing which network components were considered damaged and to what extent they were damaged. This scenario shows a critical capability of CISRM to incorporate partial component functionality and proportional resource consumption in their repair. Additionally, this failure scenario shows how the recovery results can vary when different weights are applied to the objective equation, changing the emphasis between resilience maximization and cost minimization.

Figure 11 shows three partial resilience curves of three different ω values. The lower values of ω correspond with a lower emphasis on maximizing system performance. This is demonstrated in the fact that the $\omega = 0.3$ line only reaches about 45% system performance while the $\omega = 0.9$ line reaches 100% system performance. Furthermore, Figure 12 shows the cost side of the equation for each of the three ω values, but with the meaning reversed where a lower ω puts a higher emphasis on minimizing cost. This is clearly demonstrated in Figure 12 where the $\omega = 0.3$ line has the lowest overall expenditures while the $\omega = 0.9$ line has the highest.

The three different scenarios depicted in Figures 11 and 12 can be used in a tradeoff analysis by infrastructure owners to decide what level of system performance, and by extension, overall resilience, and cost they are willing to or able to attain following a disruption. Of particular interest are the large jumps that occur between resilience and cost. For example, in Figures 11 and 12, it can be seen that when $\omega = 0.45$, a system performance of 94% can be attained at a substantially lower cost than it takes to get to a system performance of 100%.

Air Force Installation Use Case

This section will detail a potential use case for United States Air Force (USAF) Installations. One of the major challenges associated with application of flow-based network optimization models such as CISRM and the others discussed earlier is availability of reliable, real-world data (Almoghathawi & Barker, 2019). This is due to the criticality and sensitivity of much of the infrastructure systems being evaluated and the multiple system owners that would have to cooperate to generate a cohesive interdependent infrastructure network model. Additionally, in a disruptive event unfolding in real-time, restoration optimization model implementation is often hampered by the information sharing process between different CIS owners (Sharkey et al., 2015). As such, a large portion of the research and application of these models consists of evaluating historical post-disaster restoration efforts (der Sarkissian et al., 2022; Poulin & Kane, 2021; Sarker & Lester, 2019; Sharkey et al., 2016). This research proposes an alternative use case, Department of Defense installations, specifically USAF Installations.

USAF installations are the power projection platforms of that branch of the military and rely heaving on the underlying infrastructure for mission generation (Department of the Air Force, 2019). USAF civil engineering squadrons are responsible for operations and maintenance of all infrastructure systems within the installation fence line and as such, would not suffer from the same lack of oversight and cooperation that proves so challenging in many civilian application of resiliency models. A single installation could provide reliable and accurate data to construct an interdependent infrastructure network model consisting of several infrastructure layers supporting a mission generation layer. Under this construct, critical facilities for mission could be identified and their infrastructure demands quantified and isolated to reduce the computational burden of modeling the entire set of infrastructure layers. Mission owners and facility operators could then be consulted to prioritize demand criticalities and damage scenarios could be run to evaluate potential impacts to mission from infrastructure disruptions.

VI. Conclusion

Being able to adequately model CIS performance in response to disruptions is critical to identifying system interdependencies and vulnerabilities, and improving recovery planning and execution. Network flow-based optimization models are one of the most effective tools in this area of research because they are able to simulate system performance metrics such as quantities of commodities being supplied that are not able to be captured using other modeling approaches such as economic models or network topological models. Projected system response to disruptions can then be used to inform investment decisions of CIS owners who, in accordance with high-level governmental directives, are attempting to improve overall system resilience, and mitigate the economic, security, and safety impacts of CIS disruptions.

This research proposed a novel network flow-based infrastructure model and illustrated its potential applications for disaster mitigation and recovery optimization using a test network. The proposed model allows for partial functionality of system components and variable levels of critical recovery resources which have heretofore not been combined in a cohesive model. The test network used in this research was constructed to simulate a series of interconnected residential areas with electric power and water demands, and the associated multi-layer infrastructure systems to support these demands. The test network was subjected to a number of disruption scenarios including a total failure scenario in which every component of the system was rendered inoperable, a targeted attack in which system performance was monitored in response to disruption of the most critical system components, and a random failure scenario in which components were disrupted at random to simulate a natural disaster.

The total failure scenario revealed the CISRM model's superiority in prioritizing component recovery by more rapidly bringing services online and meeting consumer demand when compared to a topological-based prioritization. The targeted attack scenario revealed that removing components based on their topology (i.e., betweenness centrality in this research), was more effective at degrading system performance than the criticality determined by the CISRM model. This finding could be a result of the small size of the test network or simply an illustration of the ease of disruption compared to the more complicated system restoration. The random failure scenario displayed the potential functionality of the CISRM model as a decision-making tool by illustrating the impacts of increasing or decreasing the emphasis on system resilience as opposed to total system costs. By providing a visual showing the different levels of performance that can be achieved at different expenditures, the CISRM model could be an invaluable tool for CIS owners and operators.

Limitations

As mentioned earlier, constructing any model will always require tradeoffs between accuracy and intricacy, and complexity and computational cost. Therefore, no model is without its limitations. A limitation of the CISRM model in its current formulation is its inability to adequately capture partial performance of supply nodes. While partial functionality of a node will limit the capacity of the outgoing arcs, it does not actually reduce the available supply of commodity from the node. Additionally, the current formulation only considers three of the five types of operational interdependencies identified by Lee et al. (2007). Clearly, the research has identified several other types of interdependencies that could be included in a future formulation to create a more complete model. Furthermore, CISRM does not include a real measure of time other than as a critical resource that could be limited in a recovery scenario. Therefore, while it is useful in prioritizing recovery efforts, the current formulation lacks functionality as a scheduling model for recovery activities. A final limitation comes from the lack of real-world infrastructure data available for research. All tests performed in this research to demonstrate the capabilities of CISRM were done with notional data created for a test network, and thus CISRM has not been tested on a real-world network.

Future Research

In addition to addressing the limitations mentioned earlier, future research involving the CISRM model could be done evaluating the impacts of changing resource levels on recovery prioritizations. CISRM allows for time and money to be included as limiting resources and evaluating recovery options given a limited budget or time requirement could be useful for future CIS recovery plans. Finally, the computational cost of utilizing CISRM on a large-scale network could be significantly reduced if a future formulation were constructed in an iterative loop configuration as described in González et al. (2016). This would greatly reduce the time to successfully run a simulation but would potentially lead to a non-optimal global solution. However, this tradeoff, as described in González et al. (2016), would more accurately depict real-world operational decisions in which the best decisions are made with the currently available information, and adjusted as new information or constraints become available.

Appendix 1

Appendix 1 is associated Microsoft Excel file titled "Appendix 1 – CISRM Test Network Data". This Excel file consists of two tabs labeled "Nodes" and "Arcs" which contain the data and parameters developed for and used in this research. The column details from each tab are detailed below in Tables 2 ("Nodes") and 3 ("Arcs"). Additionally, each tab contains relevant cost data used to estimate repair costs adapted from Moore (2021). Distances used in arc calculations are notional and were generated based on the network configuration provided in the "Arcs" tab.

Table 2: Node tab column descriptions

Column	Description
A	Node number
B	Node layer
C	Node-layer combination
D	Component description
E	Node power demand (-) or supply (+)
F	Units of power demand or supply
G	Node water demand (-) or supply (+)
H	Units of water demand or supply
I	Total node repair cost in ($ K)
J	Total node repair time (units undefined)
K	Number of utility poles required to repair node
L	Quantity of power line required to repair node
M	Quantity of thick pipe required to repair node
N	Quantity of thin pipe required to repair node
O	Number of generators required to repair node
P	Number of pumps required to repair node
Q	Total node degree
R	Node out degree
S	Node in degree
T	Node betweenness centrality

Table 3: Arc tab column descriptions

Column	Description
A	Arc origin node
B	Arc destination node
C	Origin-Destination designation
D	Arc commodity
E	Arc-Commodity combination
F	Notional arc length
G	Arc power capacity
H	Arc water capacity
I	Arc flow cost for power
J	Arc flow cost for water
K	Total arc repair cost
L	Total arc repair time
M	Number of utility poles required to repair arc
N	Quantity of power line required to repair arc
O	Quantity of thick pipe required to repair arc
P	Quantity of thin pipe required to repair arc
Q	Number of generators required to repair arc
R	Number of pumps required to repair arc
S	Arc betweenness centrality

Appendix 2

Appendix 2 is an associated .txt file that contains the GAMS code generated as part of this research. The code is commented to provide an explanation of the variables and equations that do not bear the exact same notation as contained in this document.

Appendix 3

Appendix 3 is associated Microsoft Excel file titled "Appendix 3 – Test Network Scaling and Weighting Sensitivity Analysis". The file consists of three rows and four columns of graphs which show the Pareto fronts for various combinations of weighting (ω) and scaling (λ) factors. A loop was set up in GAMS to run a 10-step, total failure scenario and record the value for total system resilience and total system cost which are displayed on the y-axis and x-axis of the graphs respectively. The loop ran through each range of ω values at the indicated intervals to generate as many optimal solutions as could be found with each ω and λ combination. The top row shows Pareto fronts for ω ranging from 0-10 by 0.5 step intervals. The second row shown ω ranging from 0-1 with 0.05 step intervals. The third row shows ω ranging from 0-100 with 5 step intervals. With respect to the columns, the first column shows λ set at 500, the second columns has λ set at 1000, the third at 5000, and the fourth at 10000. This analysis was determined to be sufficient because the number and spacing of the solutions diminished as the values for each variable got higher or lower yielding the selected values of 0-1 for ω and 5000 for λ.

Bibliography

Alderson, D. L., Brown, G. G., & Carlyle, W. M. (2015). Operational Models of Infrastructure Resilience. *Risk Analysis*, *35*(4), 562–586. https://doi.org/10.1111/risa.12333

Alkhaleel, B. A., Liao, H., & Sullivan, K. M. (2022). Risk and resilience-based optimal post-disruption restoration for critical infrastructures under uncertainty. *European Journal of Operational Research*, *296*(1), 174–202. https://doi.org/10.1016/j.ejor.2021.04.025

Almoghathawi, Y., & Barker, K. (2019). Component importance measures for interdependent infrastructure network resilience. *Computers and Industrial Engineering*, *133*, 153–164. https://doi.org/10.1016/j.cie.2019.05.001

Almoghathawi, Y., Barker, K., & Albert, L. A. (2019). Resilience-driven restoration model for interdependent infrastructure networks. *Reliability Engineering and System Safety*, *185*, 12–23. https://doi.org/10.1016/j.ress.2018.12.006

Cavdaroglu, B., Hammel, E., Mitchell, J. E., Sharkey, T. C., & Wallace, W. A. (2013). Integrating restoration and scheduling decisions for disrupted interdependent infrastructure systems. *Annals of Operations Research*, *203*(1), 279–294. https://doi.org/10.1007/s10479-011-0959-3

Department of Homeland Security. (2013). *NIPP 2013 Partnering for Critical Infrastructure Security and Resilience*.

Department of the Air Force. (2019). *U.S. Air Force Infrastructure Investment Strategy (I2S)*.

der Sarkissian, R., Cariolet, J.-M., Diab, Y., & Vuillet, M. (2022). Investigating the importance of critical infrastructures' interdependencies during recovery; lessons from Hurricane Irma in Saint-Martin's island. *International Journal of Disaster Risk Reduction*, *67*, 102675. https://doi.org/10.1016/j.ijdrr.2021.102675

Dunn, S., Fu, G., Wilkinson, S., & Dawson, R. (2013). Network theory for infrastructure systems modelling. *Proceedings of the Institution of Civil Engineers: Engineering Sustainability*, *166*(5), 281–292. https://doi.org/10.1680/ensu.12.00039

Enayaty Ahangar, N., Sullivan, K. M., & Nurre, S. G. (2020). Modeling interdependencies in infrastructure systems using multi-layered network flows. *Computers and Operations Research*, *117*. https://doi.org/10.1016/j.cor.2019.104883

Filippini, R., & Silva, A. (2015). I®ML: An Infrastructure resilience-oriented modeling language. *IEEE Transactions on Systems, Man, and Cybernetics: Systems*, *45*(1), 157–169. https://doi.org/10.1109/TSMC.2014.2343751

Garay-Sianca, A., & Nurre Pinkley, S. G. (2021a). Interdependent integrated network design and scheduling problems with movement of machines. *European Journal of Operational Research*, *289*(1), 297–327. https://doi.org/10.1016/j.ejor.2020.07.013

Garay-Sianca, A., & Nurre Pinkley, S. G. (2021b). Interdependent integrated network design and scheduling problems with movement of machines. *European Journal of Operational Research*, *289*(1), 297–327. https://doi.org/10.1016/j.ejor.2020.07.013

González, A. D., Dueñas-Osorio, L., Sánchez-Silva, M., & Medaglia, A. L. (2016). The Interdependent Network Design Problem for Optimal Infrastructure System Restoration. *Computer-Aided Civil and Infrastructure Engineering*, *31*(5), 334–350. https://doi.org/10.1111/mice.12171

Haimes, Y. Y., Asce, F., Barry, ;, Horowitz, M., Lambert, J. H., Asce, M., Santos, J., Crowther, K., & Lian, C. (2005). Inoperability Input-Output Model for Interdependent Infrastructure Sectors. II: Case Studies. *Journal of Infrastructure Systems*, *11*(2), 80–92. https://doi.org/10.1061/ASCE1076-0342200511:280

Haimes, Y. Y., Asce, F., Barry, ;, Horowitz, M., Lambert, J. H., Asce, M., Santos, J. R., Lian, C., & Crowther, K. G. (2005). Inoperability Input-Output Model for Interdependent Infrastructure Sectors. I: Theory and Methodology. *Journal of Infrastructure Systems*, *11*(2), 67–79. https://doi.org/10.1061/ASCE1076-0342200511:267

Henry, D., & Emmanuel Ramirez-Marquez, J. (2012). Generic metrics and quantitative approaches for system resilience as a function of time. *Reliability Engineering and System Safety*, *99*, 114–122. https://doi.org/10.1016/j.ress.2011.09.002

Jones, R. L., Guha-Sapir, D., & Tubeuf, S. (2022). Human and economic impacts of natural disasters: can we trust the global data? *Scientific Data*, *9*(1). https://doi.org/10.1038/s41597-022-01667-x

Kivelä, M., Arenas, A., Barthelemy, M., Gleeson, J. P., Moreno, Y., & Porter, M. A. (2013). *Multilayer Networks*. https://doi.org/10.1093/comnet/cnu016

Lee, E. E., Mitchell, J. E., & Wallace, W. A. (2007). Restoration of services in interdependent infrastructure systems: A network flows approach. *IEEE Transactions on Systems, Man and Cybernetics Part C: Applications and Reviews*, *37*(6), 1303–1317. https://doi.org/10.1109/TSMCC.2007.905859

Moore, B. A. (2021). *Interdependent Infrastructure Recovery Using Multilayered Networks and Optimization*. https://scholar.afit.edu/etd/5088

National Research Council. (2012). Disaster resilience: A national imperative. In *Disaster Resilience: A National Imperative* (pp. 1–244). National Academies Press. https://doi.org/10.17226/13457

Ouyang, M. (2014). Review on modeling and simulation of interdependent critical infrastructure systems. In *Reliability Engineering and System Safety* (Vol. 121, pp. 43–60). Elsevier Ltd. https://doi.org/10.1016/j.ress.2013.06.040

Ouyang, M. (2017). A mathematical framework to optimize resilience of interdependent critical infrastructure systems under spatially localized attacks. *European Journal of Operational Research*, *262*(3), 1072–1084. https://doi.org/10.1016/j.ejor.2017.04.022

Poulin, C., & Kane, M. B. (2021). Infrastructure resilience curves: Performance measures and summary metrics. In *Reliability Engineering and System Safety* (Vol. 216). Elsevier Ltd. https://doi.org/10.1016/j.ress.2021.107926

President's Commission on Critical Infrastructure Protection. (1997). *Critical Foundations: Protecting America's Infrastructures*. https://sgp.fas.org/library/pccip.pdf

Rinaldi, S. M., Peerenboom, J. P., & Kelly, T. K. (2001). Identifying, Understanding, and Analyzing. *IEEE Control Systems Magazine*, *21*(6), 11–25.

Sarker, P., & Lester, H. D. (2019). Post-disaster recovery associations of power systems dependent critical infrastructures. *Infrastructures*, *4*(2). https://doi.org/10.3390/infrastructures4020030

Sharkey, T. C., Cavdaroglu, B., Nguyen, H., Holman, J., Mitchell, J. E., & Wallace, W. A. (2015). Interdependent network restoration: On the value of information-sharing. *European Journal of Operational Research*, *244*(1), 309–321. https://doi.org/10.1016/j.ejor.2014.12.051

Sharkey, T. C., Nurre, S. G., Nguyen, H., Chow, J. H., Mitchell, J. E., & Wallace, W. A. (2016). Identification and Classification of Restoration Interdependencies in the Wake of Hurricane Sandy. *Journal of Infrastructure Systems*, *22*(1), 04015007. https://doi.org/10.1061/(asce)is.1943-555x.0000262

Zarghami, S. A., & Gunawan, I. (2021). Graph Theory and Its Role in Vulnerability Evaluation of Infrastructure Networks. *Lecture Notes in Mechanical Engineering*, 91–101. https://doi.org/10.1007/978-3-030-64228-0_9

REPORT DOCUMENTATION PAGE

1. REPORT DATE	2. REPORT TYPE	3. DATES COVERED START DATE	3. DATES COVERED END DATE
20230323	Master's Thesis	20210901	20230323

4. TITLE AND SUBTITLE
Critical Infrastructure System Resiliency Modeling Using Multi-Layer Network Optimization

5a. CONTRACT NUMBER	5b. GRANT NUMBER	5c. PROGRAM ELEMENT NUMBER

5d. PROJECT NUMBER	5e. TASK NUMBER	5f. WORK UNIT NUMBER

6. AUTHOR(S)
Figge, Spencer, R., Captain, USAF

7. PERFORMING ORGANIZATION NAME(S) AND ADDRESS(ES)
Air Force Institute of Technology
Graduate School of Engineering and Management (AFIT/ENV)
2950 Hobson Way, Building 640
WPAFB OH 45433-8865

8. PERFORMING ORGANIZATION REPORT NUMBER
AFIT-ENV-MS-23-M-191

9. SPONSORING/MONITORING AGENCY NAME(S) AND ADDRESS(ES)
Air Force Civil Engineering Center
2261 Hughes Ave, Ste.155
JBSA Lackland, TX 78236-9853

10. SPONSOR/MONITOR'S ACRONYM(S)
AFCEC

11. SPONSOR/MONITOR'S REPORT NUMBER(S)

12. DISTRIBUTION/AVAILABILITY STATEMENT
APPROVED FOR PUBLIC RELEASE; DISTRIBUTION UNLIMITED.

13. SUPPLEMENTARY NOTES

14. ABSTRACT
Accurately modeling the interdependent operation of critical infrastructure systems is an effective and efficient way of proactively evaluating system vulnerabilities and resiliency. Infrastructure systems are designed to transport essential commodities from where they are produced to where they are consumed and network flow-based models are one of the most effective ways to simulate and quantify infrastructure performance. The literature is populated with proposed models that must balance accuracy of interdependent operations, capability to include real-world considerations, and computational cost. This research proposes an alternative network-flow based model called the Critical Infrastructure System Resiliency Model (CISRM) that focuses on modeling a subset of operational interdependencies and allows user-input damage scenarios to include partial functionality of components, restrict the available repair resources, and limit the number of work crews available to make repairs. Due to the difficulties associated with obtaining real-world infrastructure data, this research demonstrated CISRM capabilities on a notional test network. The damage scenario simulations demonstrated the superiority of CISRM in quickly restoring infrastructure services when compared to alternative restoration prioritization heuristics. The simulations also show CISRM could be a powerful decision-making tool for weighing the costs and benefits of different levels of recovery investment and the potential impact on overall system resiliency.

PREVIOUS EDITION IS OBSOLETE.

STANDARD FORM 298 (REV. 5/2020)
Prescribed by ANSI Std. Z39.18

15. SUBJECT TERMS				
16. SECURITY CLASSIFICATION OF:			17. LIMITATION OF ABSTRACT	18. NUMBER OF PAGES
a. REPORT	b. ABSTRACT	C. THIS PAGE	UU	73
U	U	U		

19a. NAME OF RESPONSIBLE PERSON	19b. PHONE NUMBER *(Include area code)*
Major Brigham A. Moore, AFIT/ENV	(937) 255-3636, ext. 4826 (brigham.moore@afit.edu)

Page 2 of 3

PREVIOUS EDITION IS OBSOLETE.

STANDARD FORM 298 (REV. 5/2020)
Prescribed by ANSI Std. Z39.18

INSTRUCTIONS FOR COMPLETING SF 298

1. REPORT DATE.
Full publication date, including day, month, if available. Must cite at least the year and be Year 2000 compliant, e.g. 30-06-1998; xx-06-1998; xx-xx-1998.

2. REPORT TYPE.
State the type of report, such as final, technical, interim, memorandum, master's thesis, progress, quarterly, research, special, group study, etc.

3. DATES COVERED.
Indicate the time during which the work was performed and the report was written.

4. TITLE.
Enter title and subtitle with volume number and part number, if applicable. On classified documents, enter the title classification in parentheses.

5a. CONTRACT NUMBER.
Enter all contract numbers as they appear in the report, e.g. F33615-86-C-5169.

5b. GRANT NUMBER.
Enter all grant numbers as they appear in the report, e.g. AFOSR-82-1234.

5c. PROGRAM ELEMENT NUMBER.
Enter all program element numbers as they appear in the report, e.g. 61101A.

5d. PROJECT NUMBER.
Enter all project numbers as they appear in the report, e.g. 1F665702D1257; ILIR.

5e. TASK NUMBER. Enter all task numbers as they appear in the report, e.g. 05; RF0330201; T4112.

5f. WORK UNIT NUMBER.
Enter all work unit numbers as they appear in the report, e.g. 001; AFAPL30480105.

6. AUTHOR(S). Enter name(s) of person(s) responsible for writing the report, performing the research, or credited with the content of the report. The form of entry is the last name, first name, middle initial, and additional qualifiers separated by commas, e.g. Smith, Richard, J, Jr.

7. PERFORMING ORGANIZATION NAME(S) AND ADDRESS(ES). Self-explanatory.

8. PERFORMING ORGANIZATION REPORT NUMBER. Enter all unique alphanumeric report numbers assigned by the performing organization, e.g. BRL-1234; AFWL-TR-85-4017-Vol-21-PT-2.

9. SPONSORING/MONITORING AGENCY NAME(S) AND ADDRESS(ES). Enter the name and address of the organization(s) financially responsible for and monitoring the work.

10. SPONSOR/MONITOR'S ACRONYM(S). Enter, if available, e.g. BRL, ARDEC, NADC.

11. SPONSOR/MONITOR'S REPORT NUMBER(S). Enter report number as assigned by the sponsoring/monitoring agency, if available, e.g. BRL-TR-829; -215.

12. DISTRIBUTION/AVAILABILITY STATEMENT. Use agency-mandated availability statements to indicate the public availability or distribution limitations of the report. If additional limitations/ restrictions or special markings are indicated, follow agency authorization procedures, e.g. RD/FRD, PROPIN, ITAR, etc. Include copyright information.

13. SUPPLEMENTARY NOTES. Enter information not included elsewhere such as: prepared in cooperation with; translation of; report supersedes; old edition number, etc.

14. ABSTRACT. A brief (approximately 200 words) factual summary of the most significant information.

15. SUBJECT TERMS. Key words or phrases identifying major concepts in the report.

16. SECURITY CLASSIFICATION. Enter security classification in accordance with security classification regulations, e.g. U, C, S, etc. If this form contains classified information, stamp classification level on the top and bottom of this page.

17. LIMITATION OF ABSTRACT. This block must be completed to assign a distribution limitation to the abstract. Enter UU (Unclassified Unlimited) or SAR (Same as Report). An entry in this block is necessary if the abstract is to be limited.

PREVIOUS EDITION IS OBSOLETE.

STANDARD FORM 298 (REV. 5/2020)
Prescribed by ANSI Std. Z39.18